

Appendix E Stress-controlled uniaxial long-term compaction

Table of content

1	Test principle	2
2	Test equipment and test set-up	3
3	Sample preparations	6
4	Execution	8
5	Post-test investigation	12
5.1	Dissolution by brine injection	12
5.2	Terminal porosity.....	12
6	Results	14
6.1	Creep compaction	14
6.2	Porosity.....	17
6.3	Permeability	23
6.3.1	Transient data for sample 1	23
6.3.2	Breakthrough pressure	24
7	Conclusions	25

1 Test principle

The experiment comprised three oedometer compaction tests with crushed salt from the Asse mine that were intended to be identical except for the initial moisture content w of the material. The adopted moisture contents for the experiment were 0 % (assumed for the state after heating over 24 hours at 105 °C), 0.1 weight percent (moisture content at delivery) and 1 % by artificial wetting.

In principle, all three tests followed the same procedure:

- installation by hand to an initial porosity of about 30 %
- measurement of the initial gas permeability¹
- step-wise mechanical loading
 - spontaneous increase of mechanical load
 - observing the axial deformation at constant load
 - measurement of gas permeability at the end of each load step¹
- step-wise temperature changes where applicable²
 - increase or decrease of temperature at constant load
- flooding with brine where applicable³
 - monitoring response in terms of deformation
- gas testing
 - measurement of gas breakthrough pressure of the flooded samples
- dismantling and measuring of the end porosity

¹ only for the oven-dry sample

² not performed for the sample with 1 % initial moisture content

³ not performed for the sample with 1 % initial moisture content as it was already at an advanced state of compaction

2 Test equipment and test set-up

Titanium test cells were developed that allowed for a permanent data acquisition during compaction including load, temperature and displacement as well as for permeability measurements during the test. The hook-ups for the permeability measurements allowed also for a later flooding of the samples. An empty open cell and a cell fully equipped for the test are depicted in Fig. 2.1.



Fig. 2.1 Test cell; left: open and empty, right: ready for the test

Each cell was then installed in a test chamber that could be heated from inside as shown in Fig. 2.2. The three chambers were then in turn installed in two frames of a universal testing machine providing the controlled mechanical load. A picture of one such frame can be seen in Fig. 2.3.



Fig. 2.2 Cell in the test chamber



Fig. 2.3 Frame of the testing machine holding two test chambers

Each frame could take only two chambers at the time but a second frame was available for the third chamber. As a result, two samples experienced the same loading history while the third one could be loaded independently. Anticipating less differences in the compaction behaviour of the dryer samples, these samples were installed in the same frame as indicated in Fig. 2.4.

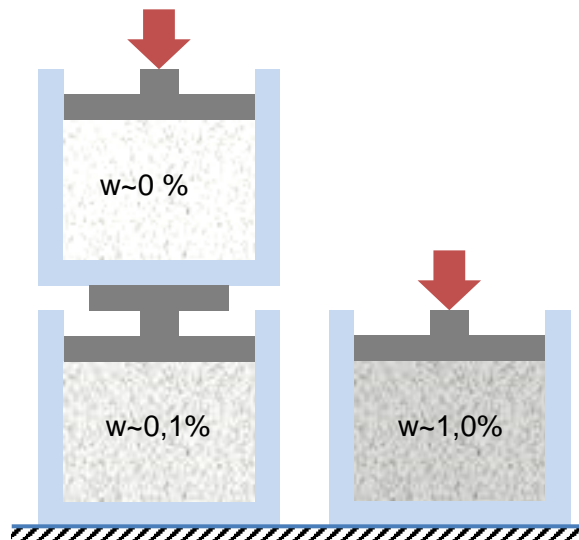


Fig. 2.4 Principle of the compaction test

3 Sample preparations

Crushed salt “table salt” z2HSSP facies from the Asse mine was used for the tests. The grain size distribution of the material was set to the specifications given in appendix G of the main report.

Preparation of the specimen was slightly different for each sample:

- sample 1
 - heating at 105 °C for 24 hours before installation
- sample 2
 - no special preparation
- sample 3
 - heating at 105 °C for 24 hours before installation
 - saturating water with salt from the sample material
 - adding red dye to the solution for later microstructural investigations⁴
 - adding solution equivalent to 1 weight percent to the sample by spraying (see Fig. 3.1)

The crushed salt material was poured into the respective test cell (see Fig. 3.2) in three layers. Each layer was compacted by hand. Characteristic data of the samples are compiled in Tab. 3.1. Then the sinter plates as well as the load piston were inserted in the cell. Finally sample 1 was flushed with nitrogen until relative humidity in the outflow became constant.

Tab. 3.1 Initial geometry and mass of the samples

Sample	Initial moisture content [%]	Diameter [mm]	Length [mm]	Mass [kg]
1	0	120	113	1,95770
2	0.1	120	107	1,8173
3	1.0	120	104	1,80215

⁴ During the project it was decided that letting the compaction test run as long as possible had priority over post-test microstructural investigations which were thus dropped



Fig. 3.1 Dyeing of the crushed salt



Fig. 3.2 Crushed salt in the test cell

4 Execution

Each of the three samples had its individual loading history due to different mechanical and thermal loads. These are summarised in Tab. 4.1 and visualised in Fig. 4.1 and Fig. 4.2.

Heating of samples 1 and 2 commenced during the load step of 13 MPa. A failure of heating in cell 1 was repaired provisionally lowering the upper temperature limit to about 60 °C. At a stress level of 18 MPa this provisional heating was switched-off again. Approaching the end of the test heating was also stopped in cell 2. The two heated samples were flooded with brine when the compaction rate had become very small during the final load step of 18 MPa.

Data were initially recorded once a minute. Because of the excessive amount of accumulated data it was later thinned out on a heuristic basis. Taking and processing samples of the extracted brine are described in detail in Appendix D of the main report. At the end of the test it was tried to determine the gas breakthrough pressure of the fully saturated samples.

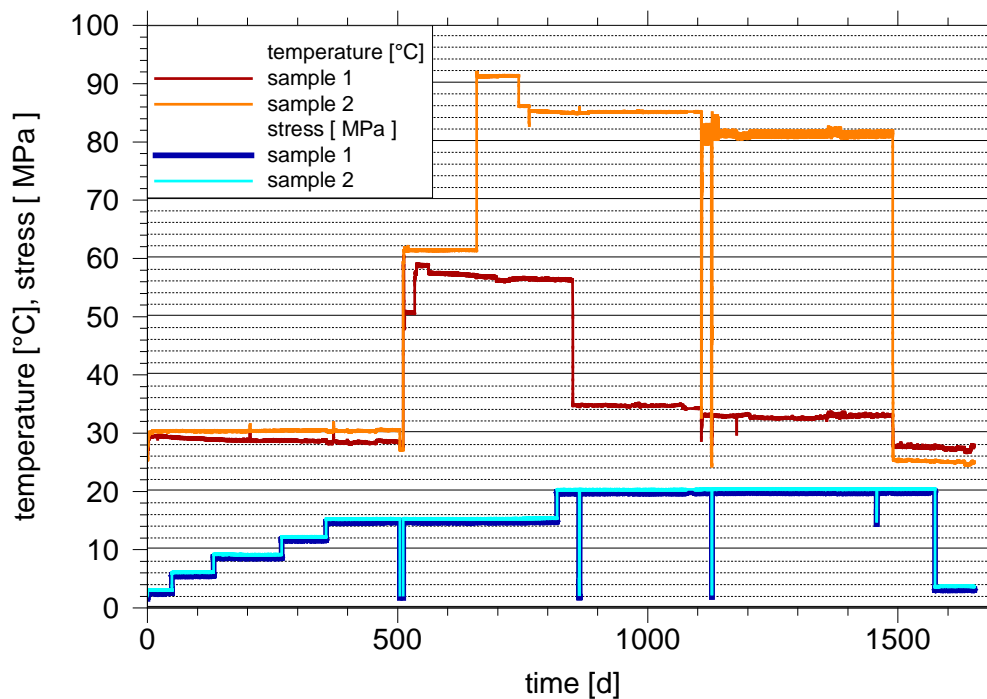


Fig. 4.1 Mechanical and thermal loading for samples 1 and 2

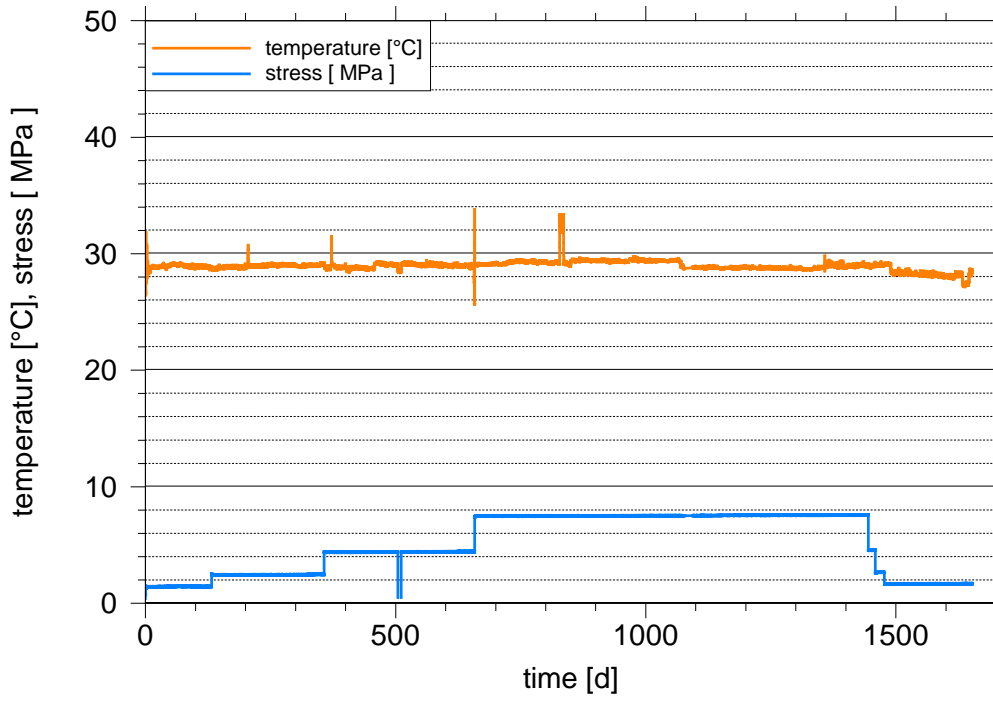


Fig. 4.2 Mechanical and thermal loading for sample 3

Tab. 4.1 Protocol of the long-term compaction tests

Date (from - to)		day (from-to)		sample 1, w=0%	sample 2, w=0.1%	sample 3, w=1.0%
22.02.2011		0		Installation and start at 1 MPa and 30 °C		
11.04.2011	12.04.2011	48	49	gas permeability measured ¹ and pressure increase to 4 MPa		
04.07.2011		132		gas permeability measured ¹ and pressure increase to 7 MPa		pressure increase to 2 MPa
17.11.2011		268		gas permeability measured ¹ and pressure increase to 10 MPa		
14.02.2012		357		gas permeability measured ¹ and pressure increase to 13 MPa		pressure increase to 4 MPa
24.04.2012		427				temporary load decrease and adjustment of position sensors
10.07.2012		504		load decrease due to failure in the testing machine		
17.07.2012		511		troubleshooting finished		
17.07.2012		511		temperature increased to 60 °C		
19.07.2012		513		heater failure		
12.08.2012		537		makeshift heater installed and temperature of 58.5 °C reached		
11.12.2012		658		gas permeability measured		pressure increase to 7 MPa
12.12.2012		659			temperature increased to 90 °C	
05.03.2013		742			temperature decreased to 85 °C	
27.03.2013		763			temperature decreased to 84 °C	
21.05.2013		818		pressure increase to 18 MPa		
21.06.2013		850		temperature decreased to 34 °C		
05.03.2014		1107		gas permeability measured ¹ temperature decreased to 25 °C unloading adjustment of position sensor pressure increase to 13 MPa temperature increased to 32 °C (sample 1) / 80 °C (sample 2)		
25.03.2014		1127		temperature decreased to 25 °C unloading exchange of position sensors		

26.03.2014		1128		pressure increase to 13 MPa temperature increased to 32 °C (sample 1) / 80 °C (sample 2)		
27.03.2014		1129		undisturbed pressure and temperature conditions restored		
15.05.2014	04.06.2014	1178	1198	flooding from below and sampling of squeezed out brine		
13.11.2014	04.12.2014	1360	1381		flooding from below and sampling of squeezed out brine	
27.01.2015	29.01.2015	1435	1437			gas permeability measured ²
06.02.2015		1445				pressure decrease to 4 MPa
20.02.2015		1459				pressure decrease to 2 MPa
10.03.2015		1477				pressure decrease to 1 MPa
23.03.2015		1490		temperature decreased to 25 °C		
07.04.2015	08.04.2015	1505	1506	gas permeability measured		
09.04.2015	17.04.2015	1507	1515		gas permeability measured	
20.04.2015	22.04.2015	1518	1520			gas permeability measured
04.05.2015	15.06.2015	1532	1574	gas permeability measured		
15.06.2015		1574		pressure decrease to 1 MPa		
03.09.2015		1654		dismantling		

¹ only oven-dry sample

² with wetted nitrogen

5 Post-test investigation

5.1 Dissolution by brine injection

Flooding of samples 1 and 2 had been prepared with considerable care to avoid solution or precipitation of solutes in the pore space of the samples. The solution was prepared from the same salt that had been used for the crushed salt samples themselves. And in case of the heated sample, the temperature of the injected solution had been raised to about the same heat level. However, to be on the safe side, samples of the injected solution as well as of the solution that was squeezed out later on were taken and analysed (see Appendix D). A comparison of the different solution samples showed, though, that the pore space was not seriously affected by the brine injection.

5.2 Terminal porosity

The porosity calculated from the displacement data for sample 3 had become negative in terms of figures during the final phase of the test. It was therefore suspected that the salt might have crept into the pores of the sinter plates at the bottom and at the top. As it turned out after dismantling, this had indeed happened to a certain extent. Between 10 and 25 g of salt were found to be lost to the sinter plates. Fig. 5.1 shows a sample right after dismantling where the stainless steel sinter plates are still attached to the salt.



Fig. 5.1 Compacted sample after dismantling, stainless steel frits still attached

The transient porosity data derived from displacement measurements thus needed to be corrected. For this purpose the terminal porosity of the samples was determined. This was achieved straight forward by measuring the amount of salt that had crept into the sinter plates. From this follows the remaining mass of compacted crushed salt between the sinter plates. By measuring the volume of the compacted sample, the bulk density was determined. After drying at 105 °C for 24 hours, the moisture content was obtained. Based on the measured data and the grain density, the terminal porosity was determined. Following this procedure it was found that the terminal porosity of all three samples was indeed positive, amounting to 1.11 %, 0.88 %, and 2.00 % for samples 1, 2, and 3, respectively.

6 Results

6.1 Creep compaction

Generally speaking, the strain rates reflect clearly changes in the loading by increasing very fast over several orders of magnitude. Some additional sample-specific features can also be observed

Sample 1

- The temperature increase to 60 °C causes a similar reaction in sample 1 as each stress increase.
- The creep accelerating effect of the load increase to 18 MPa is cancelled at 850 days by reducing the temperature from 60 °C to 35 °C.
- Flooding accelerated compaction more than any other load change.
- The two events of thermal and mechanical unloading that occurred in quick succession at day 1107 and 1127 had very little influence on further compaction.

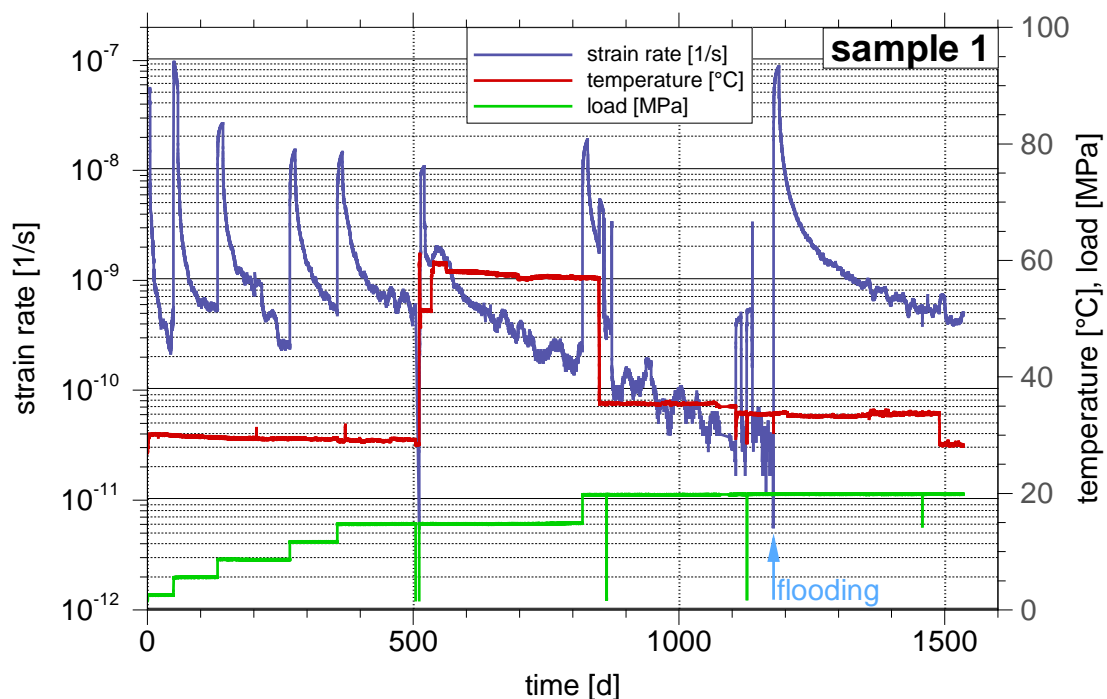


Fig. 6.1 Strain rates and loading for the oven-dry sample (sample 1)

Sample 2

- The temperature increase to 60 °C causes a similar reaction as the next temperature increase to 90 °C as well as each mechanical load increment as shown in Fig. 6.2.
- While thermal and mechanical unloading at day 1107 and 1127 had very little influence on compaction of the oven-dry sample (cf. Fig. 6.1) the impact on sample 2, by contrast, was rather dramatic as the strain rate decreased afterwards by about one order of magnitude. Interestingly, the strain rates after day 1127 were very similar in both cells despite the rather different prevailing temperature.
- Flooding accelerated compaction also in sample 2 more than any other load change.
- The temperature drop from 88 °C to 25 °C on day 1490 caused also a drop in the strain rate by almost an order of magnitude. Note that the temperature drop of about 10 °C in sample 1 (cf. Fig. 6.1) had by contrast no visible effect on the creep.

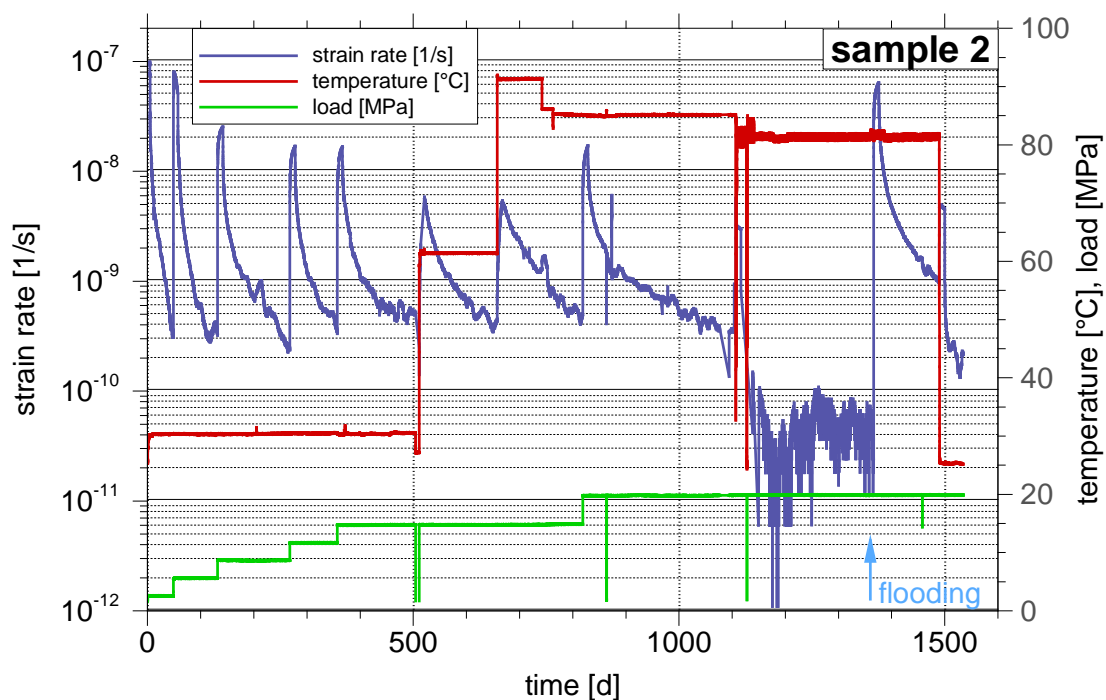


Fig. 6.2 Strain rates and loading for sample with initially 0.1 % brine (sample 2)

Sample 3

- The strain rate in the wetted sample depicted in Fig. 6.3 decreases during the first load step much slower than in the two dryer samples. This behaviour can also be observed further on (see also Fig. 6.4).
- At the end of the experiment all samples had reached a porosity between 0.88 % and 2.0% and were highly saturated with brine. The gradient of the strain rate indicating the further evolution of the respective porosity appears to be quite different, though. Sample 2 had experienced a serious temperature drop during the flooded phase and can thus hardly be compared with the other two tests. However, at about day 1420 when the porosity in sample 1 passed the value of 2 % (see dashed horizontal line in Fig. 6.6) the gradient of the strain rate was much higher than the gradient for sample 3 at the end of test.

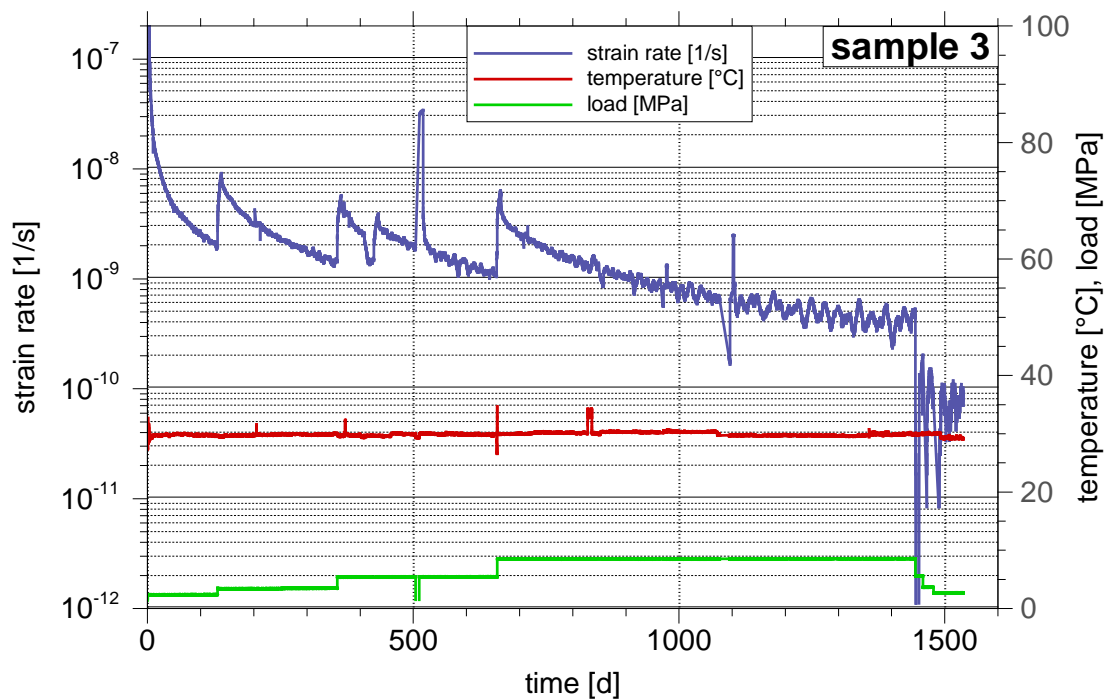


Fig. 6.3 Strain rates and loading for sample with initially 1.0 % brine (sample 3)

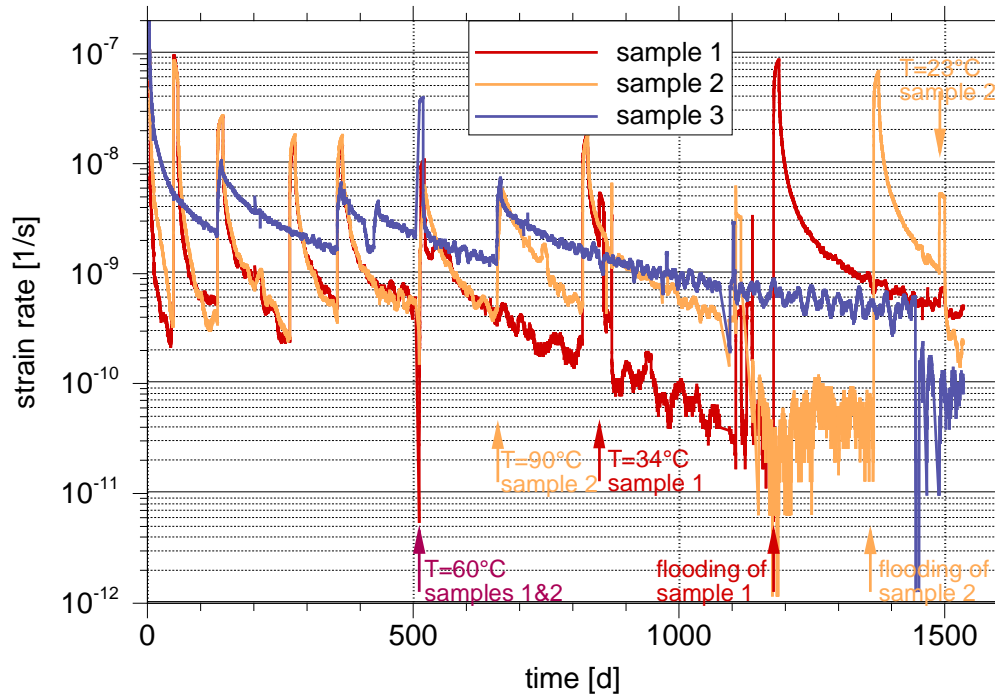


Fig. 6.4 Comparison of strain rates for all three samples

6.2 Porosity

6.2.1 Bounding curves

The exact course of the porosity evolution over time cannot be reconstructed. While it is clear that the process that leads to creep into the sinter plates is influenced by temperature and the mechanical load, it is presently not possible to quantify the referring dynamics. However, bounding curves for the true course can be found. The lower bound is given by the curve that was derived from the displacement measurements beginning with the correct initial porosity. This curve becomes increasingly too low because of the unaccounted mass loss to the sinter plates. The upper bound can thus be found by shifting the lower bounding curve upward until the correct terminal value is met. The resulting bandwidth between the bounding curves amounts to 1.11 %, 1.36 %, and 0.53 % for samples 1, 2, and 3, respectively, and is thereby satisfyingly small. The bounding curves for all three samples are compiled in Fig. 6.5. Bounding curves in the context of the loading history are depicted separately for each sample in Fig. 6.6 to Fig. 6.8.

Fig. 6.5 Bounding data for the porosity evolution for all three samples

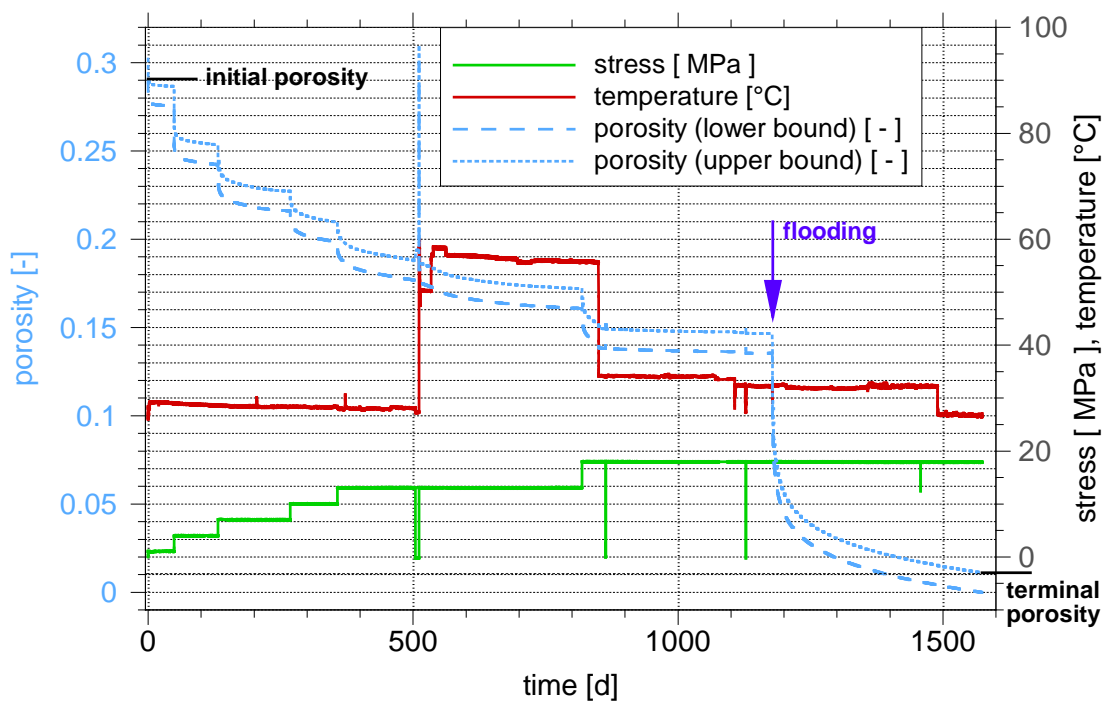


Fig. 6.6 Mechanical load, temperature and bounding porosity of the oven-dry sample

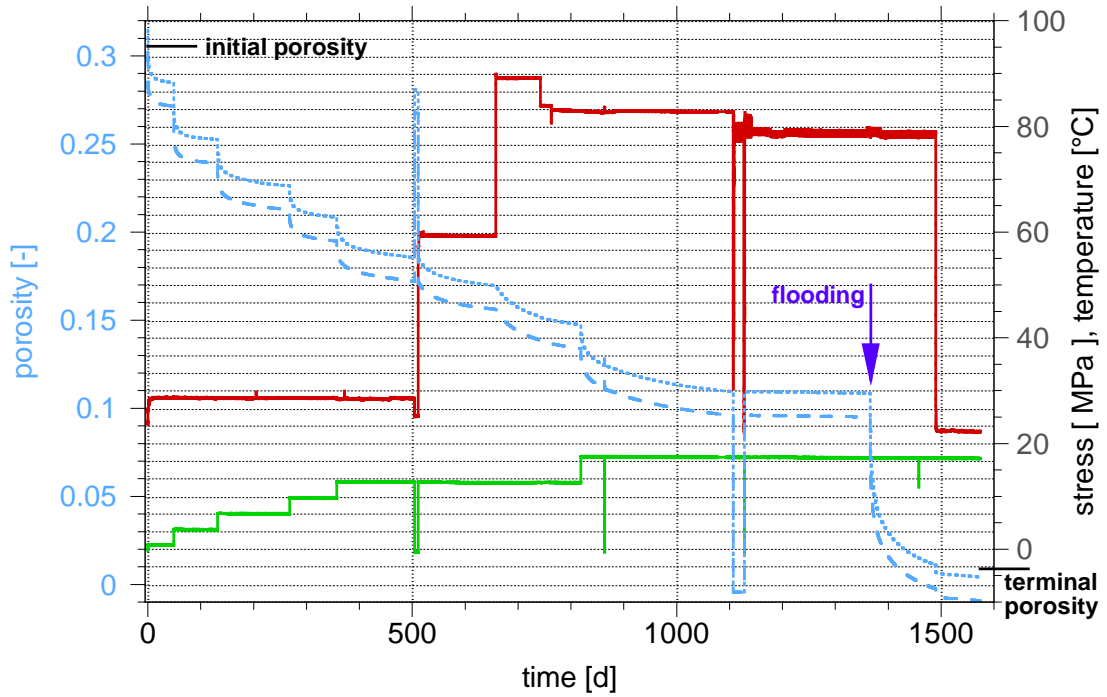


Fig. 6.7 Stress, temperature and bounding porosity of the sample with 0.1 % brine; for legend see Fig. 6.8

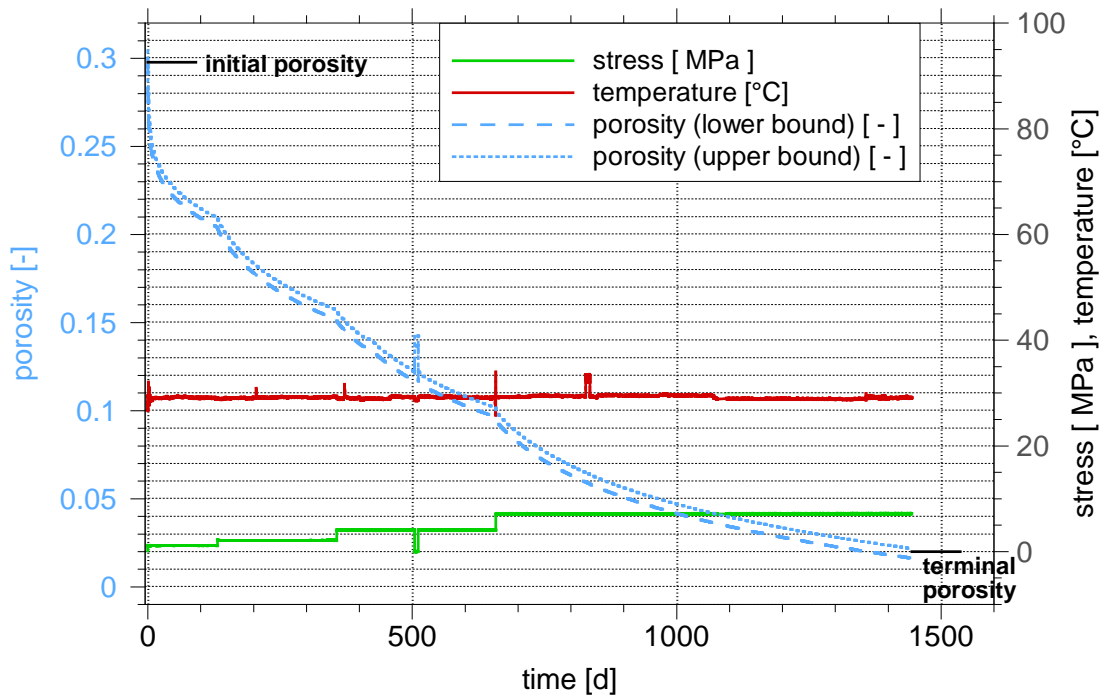


Fig. 6.8 Stress, temperature and bounding porosity of the sample with 1.0 % brine

6.2.2 Response to loading

Samples 1 and 2 experienced exclusively mechanical loading during the first 500 days which was exactly the same for technical reasons (cf. section 2). The porosity evolution was quite similar during this period (cp. Fig. 6.5). The different initial moisture contents of 0 % and 0.1 % did thus not exert a significant difference.

The initial moisture content of 1 % in sample 3 caused a rather different evolution by comparison. Despite the fact that the first load step of 1 MPa was maintained much longer than for the dryer samples 1 and 2, the strain rate of sample 3 had not yet reached nearly the low level of samples 1 and 2 when the load was eventually increased. It was thus that in case of sample 3 the following load level amounted only to 2 MPa compared to the 4 MPa in case of samples 1 and 2.

The response of the samples to loading in general (stress, heat, flooding) can be divided into two phases of different dynamics. The first phase is characterised by a very fast reduction of porosity which cannot be identified in the strain rate plots but in close-ups of the porosity evolution as shown exemplarily for sample 1 in Fig. 6.9. Data from these close-ups concerning the compaction rate during this first phase were taken and compiled in Tab. 6.1. This could be done only in an ad-hoc manner, though, because the temporal resolution of the data acquisition did not allow for deciding conclusively when this first phase ended. The values for the compaction rate given in Tab. 6.1 can thus be much higher. In general, the resulting data indicate a decreasing porosity reduction at also decreasing compaction rates.

For the same shortcomings of temporal resolution in the data it was also not possible to decide whether the first phase fades to the second one or if there is a sharp transition. It appears, though, that the transition is most pronounced in case of mechanical load changes and only hardly visible in case of flooding.

The second phase comprises a seemingly convergent reduction of the strain rate later on. A constant strain rate was not reached, however, in the experiment at any time. Only sample 3 came near to such a state at the end of the test. The strain rate plots suggest that a constant strain rate could have been reached in the long run. Due to the consolidation effect, though, the strain rate decreases continuously and cannot become con-

stant. Consolidation is higher in case of wetted salt than in case of the rather dry material.

Subsequent dynamics of porosity reduction in the second phase appear to be similar for all three types of loading. However, the strain rate seems to decrease less in case of temperature load than in case of mechanical load. Most dramatic and smoothest decrease occurs in case of flooding.

Samples 1 and 2 were flooded at 32 °C and 80 °C, respectively, and thus give some insight into the dependency of compaction after flooding on temperature. A rigorous comparison of the compaction dynamics is not possible, though, because the porosity was quite different at the beginning of flooding. But visual comparison of the porosity curves for samples 1 and 2 in Fig. 6.10 suggests that temperature seems to have secondary influence on the compaction after flooding.

6.2.3 Response to temperature decrease

Only samples 1 and 2 experienced elevated temperatures. Reducing the thermal load resulted in a significant decrease in the progress of compaction indicating hardening of the material. This applies to the dry sample (cf. Fig. 6.6 and also Fig. 6.1) as well as to the fully flooded sample (cf. Fig. 6.7 and also and Fig. 6.2).

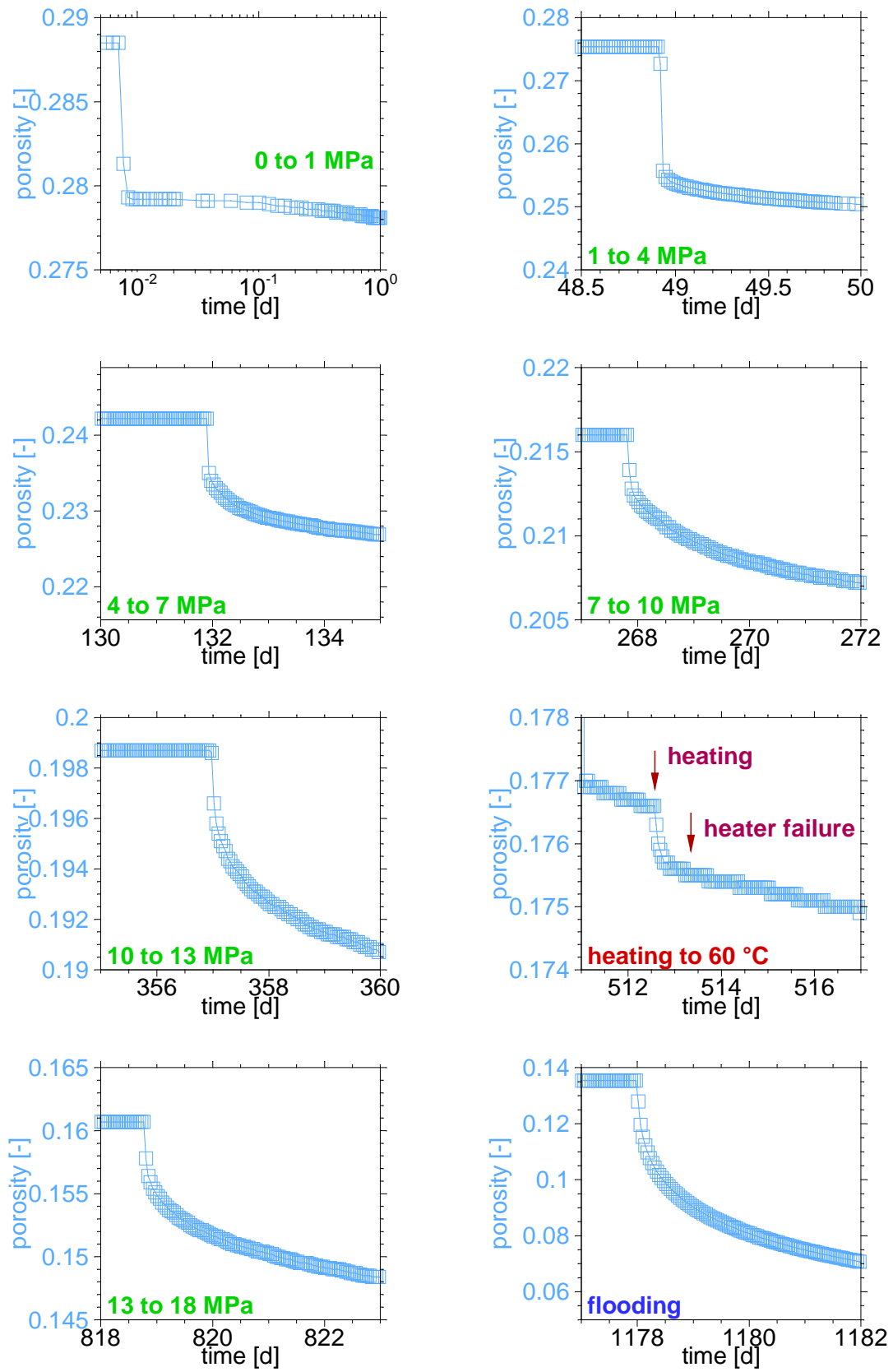


Fig. 6.9 Close-ups of the porosity evolution in the oven-dry sample (sample 1)

Tab. 6.1 Characteristic data at load changes for sample 1

Time [days]	Event	$\Delta\Phi$ [%]	Δt [d]	$\Delta\Phi/\Delta t$ [%/d]
0	Stress increase to 1 MPa	0.93	0.0015	620
48	Stress increase to 4 MPa	1.95	0.0017	1147
131	Stress increase to 7 MPa	0.71	0.041	17.3
267	Stress increase to 10 MPa	0.20	0.040	5.00
357	Stress increase to 13 MPa	0.21	0.049	4.29
512	Temperature increase to 60 °C	0.06	0.189	0.317
818	Stress increase to 18 MPa	0.29	0.043	6.74
1178	Flooding	1.55	0.09	17.2

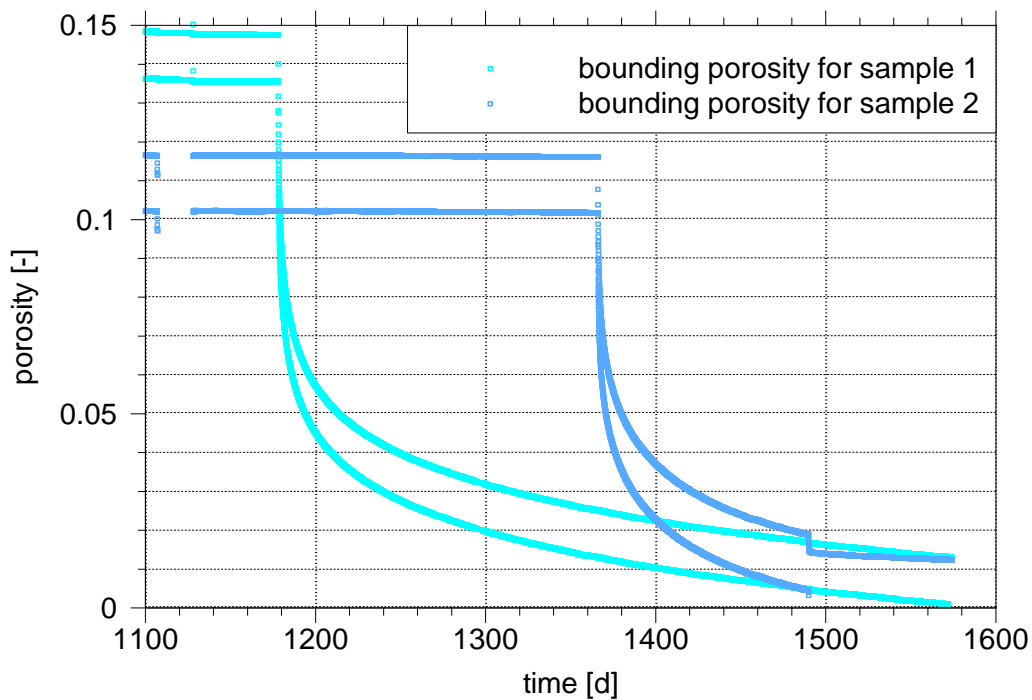


Fig. 6.10 Close-ups of the porosity evolution in sample 1 and 2

6.3 Permeability

6.3.1 Transient data for sample 1

Data for the transient gas permeability of the oven-dry sample (sample 1) are compiled in Tab. 6.2. The permeability values fit well into the bandwidth determined in the framework of phase 1 of the Repoperm-project.

Tab. 6.2 Evolution of the gas permeability of sample 1 during the dry phase

Time [d]	Porosity [%]	Injection pressure [bar]	Permeability [m ²]
11.04.2011	27.5	0,020	2,808E-12
12.04.2011	27.5	0,020	2,587E-12
04.07.2011	24.2	0,080	2,882E-12
04.07.2011	24.2	0,050	2,838E-12
04.07.2011	24.2	0,100	2,567E-12
17.11.2011	21.6	0,150	1,525E-12
17.11.2011	21.6	0,150	1,412E-12
14.02.2012	20.0	0,140	1,713E-12
14.02.2012	20.0	0,150	1,682E-12
17.07.2012	18.8	0,140	1,603E-12
17.07.2012	18.8	0,140	1,553E-12
11.12.2012	16.9	0,150	1,393E-12
11.12.2012	16.9	0,150	1,418E-12
21.06.2013	14.6	0,170	1,302E-12
05.03.2014	14.2	0,170	1,276E-12

6.3.2 Breakthrough pressure

At the end of the tests, a low gas injection pressure was applied to samples 1 and 2 and slowly increased up to 7 MPa. Neither gas nor brine outflow could be detected even at 7 MPa. Without further testing it is doubtful, though, if this value actually represents a lower bound for the air entry pressure as the salt in the sinter plates might have spoiled an accurate measurement.

7 Summary and conclusions

The experiment presented here is done in such a way that a number of aspects concerning the THM-behaviour of crushed salt during compaction is touched. Progress of stress-controlled compaction was observed on three samples. Recorded was the impact on compaction by

- different initial moisture contents
- incrementally increased mechanical load from 1 MPa up to 18 MPa⁵
- incrementally increased temperature at a mechanical load of 13 MPa
 - up to 60 °C in one step in case of sample 1
 - up to 60 °C, then to 90 °C in case of sample 2
- decrease of temperature down to 34 °C in case of sample 1
- flooding of samples 1 and 2
 - at 18 MPa, 14 % porosity and 32 °C (sample 1)
 - at 18 MPa, 10 % porosity and 80 °C (sample 2)

Additional permeability measurements were performed:

- The gas permeability of the oven-dry sample (sample 1) was measured at the end of each mechanical load step.
- At the end of the experiment it was tried to determine the air entry pressure but not achieving gas flow does not necessarily indicate a lower bound for this quantity.

Interpretation of the porosity evolution

- An initial moisture content in the order of 0.1 % does not significantly influence compaction in comparison to initially oven-dry conditions.
- Compaction of the sample with initially 1 % moisture content was much faster under much less load than compaction of the initially dryer samples.
- A temperature increase of about 30 °C had a similar effect as a mechanical load increase in the range of 3 to 5 MPa.
- Temperature decrease at maintained mechanical load results in a “hardening” of the material as the subsequent strain rate dropped considerably.

⁵ 7 MPa in case of sample 3

- The effect of flooding under high stresses can result in a loss of porosity in the order of 8 to 13 % within a year. A qualitatively similar behaviour is expected for low stresses.

Procedural conclusions

- Uncontrolled solution or precipitation in the pore space of the samples can be avoided by careful preparation of the injected brine.
- The tests were not significantly disturbed by short interruptions in applying the mechanical load like during adjustments of the displacement transducers.

All in all, the gained data thus give valuable insight into the THM-behaviour of compacting crushed salt and forms a comprehensive basis for testing related material models.